abundances for a variety of materials. The treatment decomposes secondary particle emission into two steps, i.e., ejection dynamics and electronic processes. Ejection dynamics in the selvedge govern the types of particles emitted and their atomic composition and cluster size. The origins of the particles can be traced to three dynamical processes: (i) nonreactive ejection, (ii) reactions in the selvedge, and (iii) fragmentation of clusters. Particles are emitted predominantly in the same charge state in which they exist in the material. These charge states can be modified while the emerging particle is within a few angstroms of the surface by particle–surface electronic charge-transfer transitions of the resonance or Auger type. *Emerging positive ions have a high probability of being neutralized by resonance surface-to-particle ($S \rightarrow P$) or Auger surface-to-particle ($\leftarrow S \rightarrow P$) charge-transfer transitions if the resulting neutral particle ionization potential (or vacant level in the positive ion, E_i^v) is below the Fermi level or top of the valence band of the solid. Emerging negative ions have a high probability of being neutralized by resonance particle-to-surface ($P \rightarrow S$) charge-transfer transitions if the electron affinity of the resulting neutral particle (or an occupied level of the negative ion, E_i^o) is quasi-degenerate with a vacancy in the conduction band of the solid.* The highest secondary ion yields are obtained from materials with large bands and narrow valence bands where these charge-exchange processes are improbable and the lowest ion yields are obtained from clean metals where charge-exchange processes dominate due to the broad bands. The model correctly accounts for the cluster types and their qualitative abundances observed in SIMS of metals, metal oxides, ionic salts, binary solids, and very simple molecular solids; however, as molecular size and complexity increase, the ability of the model to account for the multitudes of fragments and clusters rapidly decreases. The model is therefore proffered as a means of rationalizing and correlating SIMS results for the classes of materials described above.

Acknowledgment. This material is based upon work supported by the National Science Foundation under Grant No. CHE-7915177. We thank S. S. Ni for assistance with the SIMS of solid HCOOH and $Ni(CO)_4$.

Reversed Micelles of Aerosol-OT in Benzene. 2. Equilibrium Studies Using Vapor Pressure Osmometry and Spectrophotometry with Picric Acid as Indicator[1,2]

Kiyoshi Tamura[3] and Z. A. Schelly*

Contribution from the Department of Chemistry, The University of Texas at Arlington, Arlington, Texas 76019. *Received June 23, 1980*

Abstract: Vapor pressure osmometric results on Aerosol-OT (AOT) in benzene (with 0.03% w/w water) can best be interpreted in terms of either an empirical description or a bimodal equilibrium model. The empirical description yields only a single type of reversed micelle with mean aggregation number of $\bar{n} = 11.6$ at 25 °C and a constant monomer concentration $[A]_0 = 4 \times 10^{-4}$ M at surfactant concentrations $C_{AOT} \geq 10^{-2}$ M. $[A]_0$ may be regarded as the operational cmc of the system. The bimodal model describes aggregation by association equilibria in which a discrete monomer–6-mer–14-mer system is formed where the concentration of all species present increases with C_{AOT}. The concept of cmc is absent from this model. Spectrophotometric studies of the solubilization of picric acid indicator by AOT reversed micelle indicate that either of the two equilibrium models can serve the quantitative description of the solubilization if only a small fraction α of the micelles is eligible to accommodate picric acid in their polar interior. The solubilization equilibria lead formally to equations which suggest that the solubilization process can be regarded as adsorption of the indicator by the micelle. Numerical values of the formation constants, solubilization constants, and the α's are reported.

In a recent communication,[1] we reported preliminary concentration-jump kinetic results on the rate of solubilization of picric acid by reversed micelle of Aerosol-OT (AOT, bis(2-ethylhexyl) sodium sulfosuccinate) in benzene containing 0.03% w/w water. The faster of the two distinct rate processes observed in the millisecond range was interpreted by a two-step penetration mechanism, and the slower one was tentatively related to substrate-induced micelle formation or to the reconstruction of the indicator-containing micelles.

For the further elucidation of the mechanism of solubilization, it was necessary to obtain additional information about the physical meaning of the critical micelle concentration (cmc) for this system, the state of aggregation of AOT, and the effect of the probe molecule on the micelle formation, as well as information about the states of the picric acid probe existing in the surfactant solution.

In the present work, we report vapor pressure osmometric and spectrophotometric results on the reversed micelle of AOT in benzene, obtained in or without the presence of picric acid as indicator. The results of computer analysis of the equilibrium data are presented. The equilibrium characterization of the AOT–benzene system thus obtained is utilized in the detailed kinetic analysis of the solubilization of picric acid, described in the companion paper.[2]

Experimental Section

Chemicals. Aerosol-OT (Pflatz & Bauer, Inc.) and the solvent benzene were purified as described previously.[4] The dry benzene contains 0.03% w/w of water.[4] Picric acid (Eastman Kodak Co.) was recrystallized three times from water and dried under vacuum. All other reagents used were of reagent grade.

Spectrophotometric Measurements. The absorption spectra in the wavelength range of 280–600 nm were recorded on a Cary 219 spectrophotometer equipped with automatic base-line correction. Quartz cells of 1-cm path length were used in all experiments, thermostated at 25 °C.

Vapor Pressure Osmometry. A Hewlett-Packard Model 302B vapor pressure osmometer equipped with a variable-temperature controller was used. The instrumental calibration procedure and the method of measurements were similar to those described previously.[4] For temperature equilibration, each sample was kept in the syringe for at least 10 min

(1) Part 1 of this series: Tamura, K.; Schelly, Z. A. *J. Am. Chem. Soc.* **1979**, *101*, 7643–7644.
(2) Part 3: Tamura, K.; Schelly, Z. A. *J. Am. Chem. Soc.*, following article in this issue.
(3) R. A. Welch Postdoctoral Fellow. On leave of absence from the National Defense Academy, Yokosuka, Japan.
(4) Herrmann, U.; Schelly, Z. A. *J. Am. Chem. Soc.* **1979**, *101*, 2665–2669.

0002-7863/81/1503-1013$01.25/0

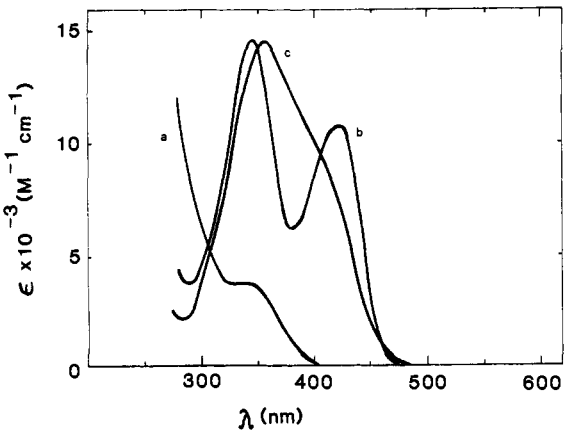

Figure 1. Absorption spectra of picric acid HP in different media at 25 °C: (a) 2.0×10^{-5} M HP in benzene; (b) 10^{-5} M HP in 10^{-2} M AOT–benzene; (c) 5.0×10^{-5} M HP in water.

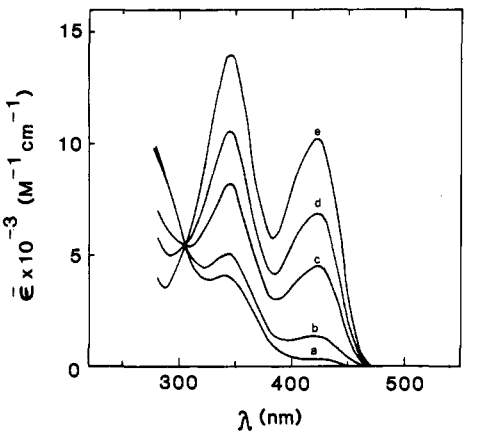

Figure 2. Effect of surfactant concentration on the absorption spectrum of 10^{-5} M picric acid at 25 °C. The AOT concentrations are as follows: (a) 6.0×10^{-5} M; (b) 2.0×10^{-4} M; (c) 6.0×10^{-4} M; (d) 10^{-3} M; (e) 2.0×10^{-3} M. $\bar{\epsilon}$ is the apparent molar decadic absorption coefficient.

before measurement. All measurements were carried out at 25 °C and repeated at least four times. Standard benzil–benzene solutions of 6×10^{-4}–1.2×10^{-2} m gave a straight line in the ΔR vs. concentration plot, and the calibration constant was determined from the slope of this line. For the surfactant solutions, in order to attain steady-state conditions, readings were taken at 2–6 min after the introduction of the samples.

Results and Discussion

Spectrophotometric Measurements. Since the current picture of solubilization by reversed micelles involves the incorporation of a substrate into distinct regions of the micelle,[5] extensive spectrophotometric measurements were carried out in order to establish the micro location as well as the states of the picric acid HP existing in AOT–benzene solution.

The absorption spectrum of picric acid HP is very sensitive to the medium. Figure 1 shows representative spectra in benzene, water, and AOT–benzene solutions. In pure benzene (Figure 1, line a), the absorption peak at 341 nm obeys the Bouguer–Lambert–Beer law in the concentration range studied ((1–5) $\times 10^{-5}$ M). This indicates that HP neither dissociates nor self-associates in benzene. The conclusion is supported also by vapor pressure osmometric measurements carried out in a much higher concentration range ((0.5–5) $\times 10^{-3}$ M) which show that HP exists only as a neutral monomer in benzene.

The spectrum of HP in water (Figure 1, line c) exhibits a single peak at 355 nm with a broad shoulder at 425 nm. The spectrum can be ascribed to the completely dissociated form of picric acid, P^-, since the addition of up to 10 equiv of NaOH has no effect on the spectrum.

The spectrum of HP in AOT–benzene solution (Figure 1, line b) somewhat resembles that in water (line c) but with two clearly separated peaks at 345 and 422 nm. The obvious difference between the two spectra (b and c), however, indicates that either the solubilized state or/and the local environment of HP in the surfactant solution is different from that in bulk water. The possibility of the sodium picrate ion pair Na^+P^- formed in the water pool of the micelle being responsible for the absorption spectrum b can be discarded since aqueous HP solutions (5×10^{-5} M) containing 0.1–5 M NaCl have spectra identical with that obtained in pure water (spectrum c). So that the effect of the local environment of HP on its absorption properties could be investigated the spectra of 5×10^{-5} M HP were taken in several different organic solvents. In highly polar solvents such as methyl alcohol, acetone, and Me_2SO, the spectra are similar to the one peak spectrum of aqueous HP solution, spectrum c. On the other hand, HP in less polar solvents such as dioxane, THF, dodecyl alcohol, and ethyl, butyl, and 1-heptyl acetates exhibits spectra similar to that obtained in AOT–benzene solution, spectrum b. It seems that in a less polar environment, HP forms a proton-transfer complex with the nucleophilic sites of the medium which

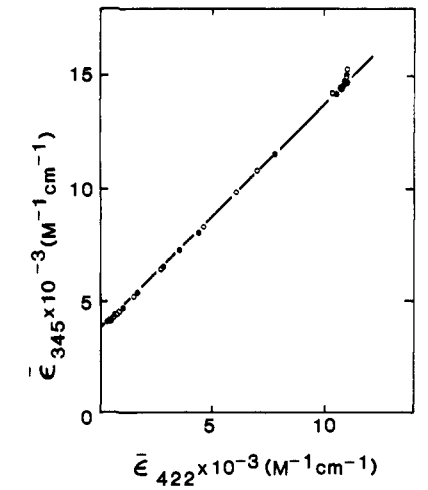

Figure 3. Relationship between the two apparent absorption coefficients $\bar{\epsilon}_{345}$ and $\bar{\epsilon}_{422}$ of the picric acid–AOT–benzene solutions at 25 °C. Open and filled circles refer to picric acid concentrations of 10^{-5} and 2.0×10^{-5} M, respectively.

is responsible for the spectrum. Possible partners in the complex formation may be the COO and SO_3^- groups of AOT or the hydration water at the interface of the micelle pool. This idea is supported by the fact that the yellow color of HP–AOT–benzene solutions (e.g., 2×10^{-5} M HP and 4×10^{-3} M AOT) disappears upon the addition of an equivalent amount of hydrochloric acid dissolved in benzene.

To investigate the question whether the two absorption peaks at 345 and 422 nm of HP–AOT–benzene solutions are caused by different species or not, we took the spectra of 10^{-5} M HP at several different AOT concentrations (Figure 2). The two absorption peak heights increase *in parallel* with one another at increasing concentration of AOT, reaching a maximum at about 2×10^{-3} M AOT. An isosbestic point is observed at 305 nm at AOT concentrations up to 2×10^{-2} M. At higher AOT concentrations, the isosbestic point is obscured due to increasing light scattering by micelles in the UV region. For solutions containing twice as much HP (2×10^{-5} M), the absorption spectra show similar trends as above but reach the saturation level at about 4×10^{-3} M AOT.

Figure 3 shows the relationship between the two absorption peak heights of HP–AOT–benzene solutions of different surfactant concentration. The linear plot of the apparent extinction coefficients $\bar{\epsilon}_{345}$ vs. $\bar{\epsilon}_{422}$ is independent of the HP concentration, and the intercept value of $\bar{\epsilon}_{345}$ (at $\bar{\epsilon}_{422} = 0$) is in agreement with the extinction coefficient of HP obtained in pure benzene. These results indicate that the two absorption peaks at 345 and 422 nm may be ascribed to the same solute species, namely to HP com-

(5) Correll, G. D.; Cheser, R. N.; Nome, F.; Fendler, J. H. *J. Am. Chem. Soc.* **1978**, *100*, 1254–1262.

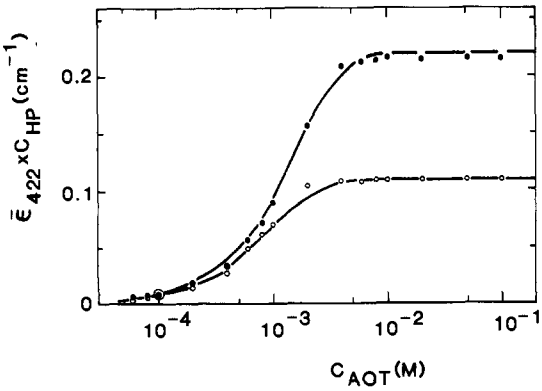

Figure 4. Concentration dependence of the absorbance per centimeter of the picric acid–AOT–benzene solutions at λ = 422 nm and 25 °C. Open and filled circles refer to picric acid concentrations of 10^{-5} and 2.0 × 10^{-5} M, respectively. The solid curves represent the calculated values obtained with use of the parameters in Table III.

Table I. Absorption Characteristics of Picric Acid in Various Media at 25 °C

medium	absorption peak: wavelength, nm	absorption peak: $10^{-3}\bar{\epsilon}$, M^{-1} cm^{-1}	isosbestic point, nm
water	355	14.6	
	425[a]		
benzene	341	3.82	
AOT–benzene	345	14.7[b]	305
	422	10.9[b]	

[a] Shoulder position. [b] Value in plateau region.

plexed through proton-transfer to its micro environment. The presence of the isosbestic point suggests that only two spectrophotometrically distinguishable forms of HP exist in AOT–benzene solutions: one is the undissociated HP in a hydrophobic environment and the other, which is responsible for the absorption peaks at 345 as well as at 422 nm, is the indicator solubilized in the polar interior of the reversed micelles.

Figure 4 shows the apparent extinction coefficient $\bar{\epsilon}_{422}$ plotted vs. the AOT concentration. At a fixed concentration of HP, the absorption increases initially with the AOT concentration and finally attains a constant value, where all HP is solubilized by the micelle. As mentioned earlier, the AOT concentration at which the absorption reaches the saturation level is directly proportional to the HP concentration; i.e., if the HP concentration is doubled, twice as much AOT is needed for complete solubilization. This important point should be kept in mind for the full appreciation of the section on Solubilization Equilibria. The absorption in the plateau region obeys the Bouguer–Lambert–Beer law. The spectrum in this range (5 × 10^{-5} M HP in 5 × 10^{-2} M AOT–benzene) is unaffected by the additional presence of 0.3 M water or 5 × 10^{-4} M NaOH. This observation indicates that at AOT concentrations corresponding to the plateau region of Figure 4, all the picric acid is solubilized by the reversed micelle in the colored form, and further that no HP is solubilized directly into the water pool even in the presence of NaOH. This conclusion is in accord with that reached for *p*-nitrophenol in AOT–heptane solution.[6] In both cases, it seems that the indicator is adsorbed at the interface of the pool where the phenolic hydroxyls are held in the proximity of the sulfonate group of the surfactant, dipping into the pool.

The absorption characteristics of picric acid are summarized in Table I.

Vapor Pressure Osmometric Results. The vapor pressure osmometric measurements were carried out on AOT–benzene solutions in the concentration range of 5 × 10^{-4}–10^{-1} M. The total concentration C of solute species was determined under the assumption that all activity coefficients were unity.[7] As shown in Figure 5, in the entire concentration range studied, the solute concentration C is much lower than the stoichiometric concentration of AOT, C_{AOT}, indicating clear evidence for micelle formation. Above 10^{-2} M AOT, the solute concentration C increases linearly with C_{AOT}, while a negative deviation from linearity is observed below this concentration.

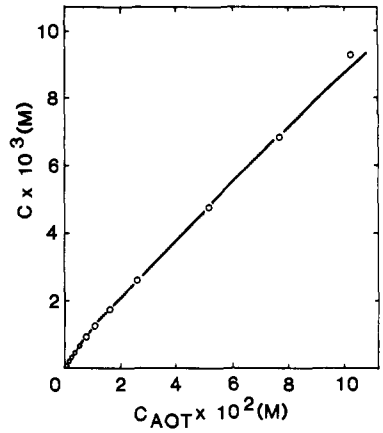

Figure 5. Total concentration of solute species in AOT–benzene solutions at 25 °C. The solid curve represents the calculated values obtained with use of the parameters in Table III for the monomer–6-mer–14-mer association model.

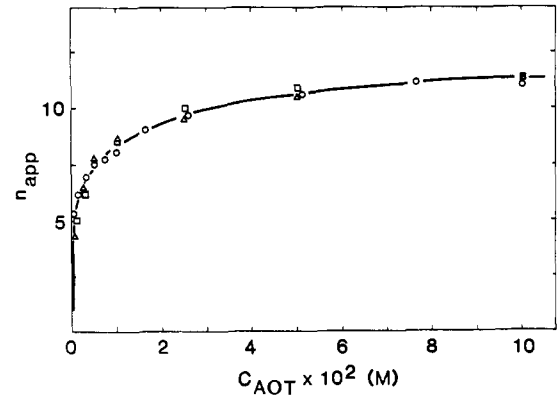

Figure 6. The apparent aggregation number n_{app} of AOT in benzene at 25 °C, with and without picric acid present. The HP concentrations are as follows: ○, no picric acid added; △, 10^{-5} M; □, 4.0 × 10^{-5} M. The solid curve represents the values calculated for the monomer–6-mer–14-mer association model with use of the formation constants in Table III.

Figure 6 shows the apparent aggregation number n_{app} (=C_{AOT}/C)[8,9] as a function of C_{AOT}, as well as the insignificant effect of the presence of HP ((1 or 4) × 10^{-5} M) on n_{app}. This latter result does not provide sufficient evidence of indicator-induced micelle formation or indicator-induced formation of merged micelles (reconstruction of the indicator-solubilizing micelles), as we tentatively proposed earlier.[1] However, due to the large excess of AOT, these possibilities cannot be excluded based solely on the vapor pressure osmometric results.

For the quantitative interpretation of the vapor pressure osmometric data, one can use two basically different methods: (a) the empirical (or graphical) method of analysis[4,8,9] and (b) the one based on the optimal choice of chemical equilibria that lead to micelle formation.[10,11]

(6) Menger, F. M.; Saito, G. *J. Am. Chem. Soc.* **1978**, *100*, 4376–4379.

(7) The assumption is a reasonable one, since the monomer AOT concentration is very low (10^{-4} M or less) and the intermolecular interaction between the aggregates is weak due to the bulky hydrophobic exterior of the micelles.

(8) Kon-no, K.; Kitahara, A. *Kogyo Kagaku Zasshi* **1965**, *68*, 2058–2061.

(9) Kon-no, K.; Kitahara, A. *J. Colloid Interface Sci.* **1971**, *35*, 636–642.

(10) Lo, F. Y. F.; Escott, B. M.; Fendler, E. J.; Adams, E. T., Jr.; Larsen, R. D.; Smith, P. W. *J. Phys. Chem.* **1975**, *79*, 2609–2621.

Table II. Operational cmc Value and Mean Aggregation Number $\bar{n}$ of AOT in Benzene

temp, °C	cmc, 10^{-3} M	$\bar{n}$	method of measurement[a]	ref
20	0.5		spec conduc	12
20	0.9		iodine spectra	13
20	2.0		TCNQ spectra	13
22	2.2		positron annihil	14
25	0.4	11.6	vap press osm	*b*
25	0.7		AO-base spectra	4
25		14.8	vap press osm	12
28	2.8	23	light scatt	15
37		10	vap press osm	4
37	2.3	18	vap press osm	8
40		13.6	vap press osm	9

[a] Key: spec conduc, specific conductance; positron annihil, positron annihilation; vap press osm, vapor pressure osmometry; light scatt, light scattering. [b] This work; empirical method.

(a) Empirical Method. The stoichiometric concentration of surfactant C_{AOT} may be expressed in terms of the concentration of monomer surfactant [A] and the concentration [M] or micelle $A_{i\neq1}$ of mean aggregation number $\bar{n}$ as

$$C_{AOT} = [A] + \bar{n}[M] \quad (1)$$

and the total solute concentration C as

$$C = [A] + [M] \quad (2)$$

By combining eq 1 and 2, we obtain

$$C = [A] + (C_{AOT} - [A])/\bar{n} = (1 - 1/\bar{n})[A] + C_{AOT}/\bar{n} \quad (3)$$

If one assumes $\bar{n}$ and [A] are constants, independent of C_{AOT} in the domain corresponding to the linear portion of the curve in Figure 5, the linear portion of the curve can be described by eq 3. Thus, the experimental curve can be used for the determination of $\bar{n} = 11.6$ and $[A]_0 = 4 \times 10^{-4}$ M. The symbol $[A]_0$ is used for [A] in the linear range. These values can be compared with the ones reported in the literature,[4,8,9,12-15] which are summarized in Table II. The similarity between $\bar{n} = 11.6$ (25 °C) and $\bar{n} = 10$ (at 37 °C, reported earlier)[4] indicates only a weak temperature dependence of the aggregation. The $[A]_0$ value, that can be regarded as the operational cmc of the system, is comparable to the value 7×10^{-4} M obtained by a spectrophotometric method using acridine orange base as indicator[4] as well as to the one obtained through conductivity measurements (5×10^{-4} M at 20 °C).[12] Nevertheless, as can be seen in Figure 5, the deviation from linearity reaches up to $C_{AOT} = 10^{-2}$ M, a much higher concentration than the graphically obtained value of $[A]_0$. Since information on the concentration range below 10^{-2} M AOT is especially important for the interpretation of the solubilization kinetics,[2] one may consider to extend the assumption of $\bar{n}$ = constant = 11.6 also for the nonlinear range, which then allows the calculation of [A] and [M] (by eq 1 and 2) in the entire concentration range studied. The micelle concentration thus obtained is proportional to C_{AOT} and can be expressed by the empirical equation $[M] = C_{AOT}/11.7$ for all surfactant concentrations, including both the linear and nonlinear ranges. The monomer concentration [A] increases with C_{AOT} in the low concentration range and finally attains a constant value $[A]_0$ at about 10^{-2} M AOT.

The above data treatment has both positive and negative features. Its attractiveness lies in the fact that it provides a description similar to that of the familiar "normal" aqueous micelle systems: a concentration independent $\bar{n}$ and $[A]_0 \approx$ cmc. Also, the constant $\bar{n}$ may imply a monodisperse size distribution which is in agreement with results obtained for the AOT–benzene system by light-scattering[16] and ultracentrifugation[17] methods. The major weakness of the graphical treatment, however, is the lack of any relationship between the method and the existence of chemical equilibria that lead to micelle formation, as expressed by the mass action law.

(b) Multiple-Equilibrium Method. The application of this method involves the assumption of simple, micelle-producing aggregation equilibria, together with simplifying assumptions about the values of the equilibrium constants. On the basis of these assumptions, the concentration of the individual aggregates $[A_i]$ can be calculated and compared with the experimental value of C_{AOT} and C through eq 4 and 5, where i is the aggregation number.

$$C_{AOT} = \sum_i i[A_i] \quad (4)$$

$$C = \sum_i [A_i] \quad (5)$$

The comparison allows the selection of a best equilibrium model.

In the following we describe the models we tested.

(1) Infinite Successive Self-Association Models. Since this model may involve an infinite number of successive association constants, $K_{i(i+1)}$ (eq 6), for any practical calculation, simplifying

$$\begin{aligned} 2A &\rightleftharpoons A_2 \quad K_{12} \\ A_2 + A &\rightleftharpoons A_3 \quad K_{23} \\ &\vdots \\ A_i + A &\rightleftharpoons A_{i+1} \quad K_{i(i+1)} \\ &\vdots \end{aligned} \quad (6)$$

assumptions must be made. Therefore, we confined our analysis to five types of association, the first four of which have been discussed previously.[10]

(i) All species A_i are assumed to be present with all formation constants equal, i.e., $K_{12} = K_{23} = K_{34} = \ldots$.

(ii) Species with odd aggregation number are absent, and the formation constants of the even-numbered species are equal, i.e., $K_{12}^2 = K_{24} = K_{46} = \ldots$.

(iii) All species are present and all formation constants are equal, except for that of the dimer, i.e., $K_{12} \neq K_{23} = K_{34} = \ldots$.

(iv) Species with odd aggregation number are absent, and the formation constants of the even-numbered species are equal, except for that of the dimer, i.e., $K_{12}^2 \neq K_{24} = K_{46} = \ldots$.

(v) All species are present, but the formation constant of the dimer is different from that of the odd-numbered species (which are equal among themselves), as well as of the even-numbered species (equal among themselves), i.e., $K_{12} \neq K_{23} = K_{45} = \ldots \neq K_{34} = K_{56} = \ldots$.

(2) Finite Successive Self-Association Models. These models are similar to those in 1, but it is assumed that the aggregation number i is finite, i.e., the micelles have a certain limit for accommodating surfactant molecules. In this group we tested four models that correspond to the assumptions given in (i)–(iv) for infinite association.

(3) The Monomer–*n*-Mer Association Model. This (see eq 7)

$$nA \rightleftharpoons A_n \quad K \quad (7)$$

assumes that only monomer and n-mer are present at significant concentration.

(11) (a) Kertes, A. S.; Gutmann, H.; Levy, O.; Markovits, G. Y. In "Chemie, Physikalische Chemie und Anwendungstechnik der Grenzflächenaktiven Stoffe", Proceedings of the 6th International Conference on Surface Active Substances; Carl Hanser Verlag: Munich, 1973; pp 1023–1033. (b) Markovits, G. Y.; Levy, O.; Kertes, A. S. *J. Colloid Interface Sci.* **1974**, *47*, 424–430. (c) Gutmann, H.; Kertes, A. S. *Ibid.* **1975**, *51*, 406–411. (d) Kertes, A. S.; Gutmann, H. In "Surface and Colloid Science"; Matijevic, E., Ed.; Wiley: New York, 1976; Vol. 8, pp 193–295.

(12) Eicke, H. F.; Arnold, V. *J. Colloid Interface Sci.* **1974**, *46*, 101–110.

(13) Muto, S.; Meguro, K. *Bull. Chem. Soc. Jpn.* **1973**, *46*, 1316–1320.

(14) Jean, Y.; Ache, H. J. *J. Am. Chem. Soc.* **1978**, *100*, 984–985 and 6320–6327.

(15) Kitahara, A.; Kobayashi, T.; Tachibana, T. *J. Phys. Chem.* **1962**, *66*, 363–365.

(16) Siegel, L. A. *J. Chem. Phys.* **1958**, *29*, 1091–1096.

(17) Peri, J. B. *J. Colloid Interface Sci.* **1969**, *29*, 6–15.

Table III. Equilibrium Parameters for Micelle Formation and for Solubilization of Picric Acid in AOT–Benzene at 25 °C

aggregation numbers of the species A_m and A_n	$m = 6$	$n = 14$
micelle formation constants	$K_1 = 1.1 \times 10^{24}$	$K_2 = 7.2 \times 10^{59}$
solubilization constants	$K_{s1} = 3.6 \times 10^5$	$K_{s2} = 7.7 \times 10^7$
fraction of micelles eligible for solubilization	$\alpha_1 = 0.064$	$\alpha_2 = 0.095$

(4) Bimodal Association Model (monomer–*m*-mer–*n*-mer). In this model[11] (see eq 8) it is assumed that two distinct aggregation

$$mA \rightleftharpoons A_m \quad K_m \qquad nA \rightleftharpoons A_n \quad K_n \tag{8}$$

numbers are favored by the system such that $2 \leq m < n$.

All 11 models were tested on computer by interating the adjustable parameters $K_{i(i+1)}$ and i and computing the concentrations of the individual aggregates $[A_i]$ for a given surfactant concentration C_{AOT}. Then, C was calculated by using eq 5 and compared with the experimentally observed value. The computations were carried out for several different surfactant concentrations (covering the whole concentration range studied), and the adjustable parameters were optimized by minimizing the relative standard deviation $\bar{\sigma}$ between the computed and observed values of C.

None of the infinite self-association models (1) can be fitted to the experimental results. Even the best case, the type v association, has $\bar{\sigma} = 26\%$. The finite self-association models (2) are somewhat better. The best case is the association of type (iii) with maximum aggregation number $i = 13$. Here $\bar{\sigma} = 6.7\%$. For model 3, the best result is obtained for $n = 10$, with $\bar{\sigma} = 13\%$.

The overall best result is obtained with use of the bimodal association model 4. With the optimal values of $m = 6$ and $n = 14$, the relative standard deviation is only $\bar{\sigma} = 3.8\%$. The computed C and n_{app} values are shown as solid lines in Figures 5 and 6, respectively. Both are in excellent agreement with the experimental results. The equilibrium and solubilization parameters (discussed in the next section) are summarized in Table III. The relative stability of the 6-mer and 14-mer can be estimated by comparing the mean association constants of the successive steps leading to their formation, defined as $\bar{K}_6 = K_m^{1/(m-1)} = K_6^{1/5}$ and $\bar{K}_{14} = K_n^{1/(n-1)} = K_{14}^{1/13}$, respectively. $\bar{K}_6$ is found to be 6.4×10^4, somewhat greater than $\bar{K}_{14} = 4.0 \times 10^4$, indicating that the surfactant molecule in the 6-mer is slightly more stable than that in the 14-mer. At this point one might speculate that the polar head groups possibly have an octahedral-like geometrical arrangement in the 6-mer, and a face-centered-cubic-like arrangement in the 14-mer.

Figure 7 shows the computed values of the monomer, 6-mer, and 14-mer equilibrium concentrations as a function of the surfactant concentration C_{AOT}. In this picture, [A] is not constant and its value is smaller by about 1 order of magnitude than the $[A]_0$ value, which was identified earlier as the operational cmc by using the empirical graphical method. Although the concept of the (operational) cmc is absent from the bimodal distribution model, interestingly, the experimentally found breaks in several observed physical quantities[4,12-15] (which are utilized to indicate the onset of micelle formation; see Table II) fall in the surfactant concentration range where $[A_6]$ and $[A_{14}]$ apparently start to reach levels detectable by the individual methods.

The bimodal distribution model has been successfully used previously for the description of the association of several alkylammonium inorganic salts in nonpolar solvents.[11] The actual distribution in such systems is probably not discrete but rather clustered *around* the two favored aggregation numbers.

Solubilization Equilibria. Similar to the analysis of the vapor pressure osmometric results, several models were considered also for the interpretation of the optical absorption of AOT–benzene–HP solutions. The quality of the individual models was tested by their ability to simulate the experimental absorbances at $\lambda = 422$ nm as a function of the surfactant concentration (Figure 4). Since the description of the solubilization must be in accord with the equilibrium description of the AOT–benzene system, the solubilization models considered are related to either

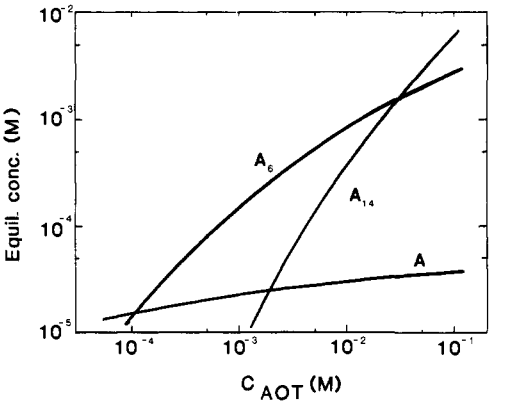

Figure 7. Equilibrium concentrations of the monomer, 6-mer and 14-mer, computed by using the bimodal association model of AOT in benzene at 25 °C.

the empirical (single micelle) or the bimodal micellization pictures.

(a) Empirical Description. Here, with only one kind of micelle M ($\bar{n} = 11.6$) present in the solution, the overall solubilization equilibrium of picric acid HP can be written as eq 9 where K_s is

$$M + HP \rightleftharpoons M{\cdot}HP \quad K_s \tag{9}$$

the solubilization constant, and M·HP is the species responsible for the yellow color of AOT–benzene–HP solutions. The optical absorption per cm, $D = \bar{\epsilon}[M{\cdot}HP]$ at $\lambda = 422$ nm, can be calculated by using the known value of $\bar{\epsilon} = 1.09 \times 10^4$ M^{-1} cm^{-1} (Table I), and the equilibrium value of [M·HP], computed from assumed values of K_s. However, in order to be able to simulate the sigmoid concentration dependence of the absorption (Figure 4), one is compelled to assume that only a fraction α of the micelles is eligible to solubilize HP. Then, if at given HP and AOT concentrations the fraction Θ of the eligible micelles is actually solubilizing picric acid, the equilibrium constant is given by an expression (eq 10)

$$K_s = \Theta/(1 - \Theta)[HP] \tag{10}$$

that is analogous to the Langmuir adsorption isotherm where [HP] is the equilibrium concentration of the free picric acid, which is its initial concentration $[HP]_0$ minus [M·HP]. Since the equilibrium concentration of the colored species is $[M{\cdot}HP] = \alpha[M]\Theta$, it can also be expressed in terms of α and K_s as eq 11. The optimal

$$[M{\cdot}HP] = \alpha[M]K_s[HP]/(1 + K_s[HP]) \tag{11}$$

values of the adjustable parameters are found to be $\alpha = 0.10$ and $K_s = 6.8 \times 10^5$ M^{-1}.

As an alternative treatment, in analogy with the Freundlich adsorption isotherm, the expression for the solubilization constant can be written as eq 12 where the subscript f refers to Freundlich

$$K_f = [M{\cdot}HP]/[M][HP]^{1/q} \tag{12}$$

and q is an empirical constant. The absorption data in Figure 4 can be described also by eq 12, if $K_f = 0.66$ and $q = 6$. In this connection it is interesting to note that, in general, for adsorption from solution, the variation of the extent of adsorption with the concentration of solute is usually represented by the Freundlich adsorption isotherm.[18] Anyhow, our results suggest that the solubilization of picric acid into reversed micelles of AOT may be considered as an adsorption phenomenon. Furthermore, since the Freundlich equation corresponds to adsorption of molecules to a nonuniform surface,[19] our results may indicate that AOT reversed micelles are nonuniform in their solubilization properties. An expression for the nonuniformity of the solubilizing sites may be the parameter α that we were forced to introduce in the derivation of eq 11. As to the nature of the nonuniformity, one has to consider the possible reasons which enable only a small fraction

(18) Maron, S. H.; Prutton, C. F. "Principles of Physical Chemistry", 4th ed.; Macmillan: New York, 1965; Chapter 20.

(19) Halsey, G. D., Jr. In "Advances in Catalysis and Related Subjects"; Frankenburg, W. G., Komarewsky, V. I., Rideal, E. K., Eds.; Academic Press: New York, 1952; Vol. 4, pp 259–269.

α of the micelles to solubilize picric acid. Clearly, the few eligible micelles may differ from the majority in shape and physical size. The differences may arise due to fluctuations in water content and aggregation number.

(b) Bimodal Solubilization. In this description it is assumed that both the 6-mer and the 14-mer can incorporate HP

$$A_6 + HP \rightleftharpoons A_6{\cdot}HP \quad K_{s1} \tag{13}$$

$$A_{14} + HP \rightleftharpoons A_{14}{\cdot}HP \quad K_{s2} \tag{14}$$

where $A_6{\cdot}HP$ and $A_{14}{\cdot}HP$ are the colored species, with identical spectroscopic properties. Similar to the situation discussed in the preceding section, in order to be able to simulate the experimental results in Figure 4, again one is forced to assume that only a fraction α_1 of A_6 and a fraction α_2 of A_{14} are eligible for solubilization. Then, equations can be written for K_{s1} and K_{s2}, as well as for $[A_6{\cdot}HP]$ and $[A_{14}{\cdot}HP]$, similar to eq 10 and 11, respectively. The solid curve in Figure 4 was computed by using the optimal values of the adjustable parameters that are summarized in Table III. An equally good fit can be obtained if one assumes $\alpha_1 = \alpha_2$, but such a condition is difficult to justify physically.

Alternate models, in which the idea of fractional eligibility for solubilization is substituted by other hypotheses, were also tested, unsuccessfully. For example, none of the following assumptions or combinations thereof leads to acceptable results: (i) only one type of micelle, the 6-mer or the 14-mer, can solubilize HP; (ii) both types can solubilize picric acid, but only one of the products, $A_6{\cdot}HP$ or $A_{14}{\cdot}HP$, contributes to the optical absorption in the visible range; (iii) both micelle types can solubilize HP, but an indicator-induced micelle formation (eq 15) takes place simul-

$$lA + HP \rightleftharpoons A_l{\cdot}HP \tag{15}$$

taneously, where $l \neq m,n$; (iv) the solubilization process involves the substitution of HP for a surfactant monomer (e.g., eq 16).

$$A_m + HP \rightleftharpoons A_{m-1}{\cdot}HP + A \tag{16}$$

With reference to the optimal values of the parameters found for the bimodal solubilization model (Table III), the results indicate that picric acid is more stable in the 14-mer than in the 6-mer ($K_{s1} \ll K_{s2}$) and that a larger fraction of the 14-mer is eligible for solubilization than the 6-mer ($\alpha_1 < \alpha_2$).

Summary

The investigation of Aerosol-OT reversed micelle in benzene reveals that the equilibrium behavior of the system can be best characterized either by an empirical description as a monomer (single) micelle association (where the mean aggregation number of the micelle is $\bar{n} = 11.6$) or by a bimodal monomer-6-mer-14-mer equilibrium model. The experimental results indicate that, in agreement with findings on similar systems,[11a] aggregation starts already at surfactant concentrations as low as 10^{-6}-10^{-5} M. According to the empirical description, the monomer concentration has a constant value of $[A]_0 = 4 \times 10^{-4}$ M at surfactant concentrations of $C_{AOT} \geq 10^{-2}$ M. In this picture, $[A]_0$ can be regarded as the operational cmc of the system. The concept of the operational cmc is absent from the bimodal equilibrium model, where the concentration of all species present increases with C_{AOT}. In contrast to the bimodal model, the single micelle description cannot be quantitatively related in a simple way to any association equilibria that may lead to micelle formation.

Either of the two micelle formation models can serve as the basis for the quantitative description of the solubilization of picric acid in AOT-benzene reversed micelles, where only a small fraction of the aggregates is eligible to accept the substrate. The fractional eligibility can be understood in terms of a multidimensional distribution, where only micelles with a certain aggregation number, pool size, and perhaps shape may accommodate picric acid. The solubilization equilibria formally led to expressions that indicate that the solubilization process can be regarded as adsorption of picric acid by the micelle.

Acknowledgment. This work was partially supported by the Robert A. Welch Foundation and the Organized Research Fund of UTA. Acknowledgment is made to the donors of the Petroleum Research Fund, administered by the American Chemical Society, for partial support of this research.

Reversed Micelle of Aerosol-OT in Benzene. 3. Dynamics of the Solubilization of Picric Acid[1,2]

Kiyoshi Tamura[3] and Z. A. Schelly*

Contribution from the Department of Chemistry, The University of Texas at Arlington, Arlington, Texas 76019. *Received August 7, 1980*

Abstract: Concentration-jump kinetic results on the penetration of picric acid probe molecules into reversed micelles of Aerosol-OT in benzene (containing 0.03% w/w water) reveal the presence of at least four distinct rate processes. One of the relaxation times is in the submillisecond and the others are in the millisecond range. A physical interpretation is presented which is in agreement with the equilibrium descriptions of the system. The formal kinetic treatment allows the computation of the rate parameters which provide the best fit with the experimental results. Numerical values of most of the rate and equilibrium constants involved are reported.

In a recent paper,[1] we reported preliminary results on the kinetics of the penetration of picric acid probe molecule into reversed micelle of Aerosol-OT in benzene. Aerosol-OT (AOT, bis(2-ethylhexyl) sodium sulfosuccinate) is a typical anionic surfactant that forms reversed micelle in apolar solvents. Reversed micelles can be characterized as aggregates of amphiphilic molecules, with their polar head groups concentrated in the interior of the aggregates while their hydrophobic groups extend into the surrounding apolar solvent. The polar head groups may dip into a water pool that usually forms the core of the micelle. Either the water originates from the solvent (where a small amount remains even after careful drying) or it is added on purpose.

Picric acid is colorless in benzene, but it turns yellow when it reaches the polar interior of the reversed micelle after mixing.

(1) Part 1: Tamura, K.; Schelly, Z. A. *J. Am. Chem. Soc.* **1979**, *101* 7643-7644.
(2) Part 2: Tamura, K.; Schelly, Z. A. *J. Am. Chem. Soc.*, preceding paper in this issue.
(3) R. A. Welch Postdoctoral Fellow. On leave of absence from the National Defense Academy, Yokosuka, Japan.

0002-7863/81/1503-1018$01.25/0